Grafted Polymer Brushes: A Constant Surface Pressure Molecular Dynamics Simulation

Gary S. Grest

Corporate Research Science Laboratories, Exxon Research and Engineering Company, Annandale, New Jersey 08801

Received July 22, 1993; Revised Manuscript Received November 1, 1993®

ABSTRACT: A constant-pressure molecular dynamics simulation of polymeric brushes in solvents of varying quality is presented. In contrast to previous simulations on polymer brushes, the surface osmotic pressure Π_a is fixed and the grafting density is allowed to vary as a function of chain length N and solvent quality. In a good solvent, the brush height $h \sim N\rho_a^{1/3}$ and Π_a scales as $N\rho_a^x$ with $x = 2.5 \pm 0.2$ where N is the chain length and ρ_a is the grafting density. This is in contrast with scaling theories in which $x = {}^{11}/_{6}$ and self-consistent mean field theories in which $x = {}^{5}/_{3}$. In a Θ solvent, $x = 3.0 \pm 0.2$, while both theories give $x = 2$. For fixed Π_a, the brush height h was found to be nearly independent of solvent quality. Results for fixed grafting sites and for annealed chains in which the tethered end of the chain is free to move within the grafting plane are presented.

I. Introduction

Polymers near a surface have been the subject of intense study, particularly in the past 6 or 7 years.[1] This interest has arisen for several reasons. One is that polymers either grafted or adsorbed on a surface have important technological applications in many areas, including colloidal stabilization[2] and lubrication. These systems are also of interest since the confinement of a chain near a surface leads to configurations which are qualitatively different from those of free chains. While both adsorbed polymers and end-grafted polymers display interesting phenomena near the surface, the properties of end-grafted chains are somewhat easier to understand. The reason is twofold. The first is that end-grafted chains equilibrate more readily and are less likely to get trapped in nonequilibrium configurations due to kinetic effects, though they do exist. The second reason is that polymer chains under conditions of strong stretching can be understood to first order by relatively simple scaling and free-energy balance arguments. Using such arguments, Alexander[3] and de Gennes[4] showed that the brush height h and the end-to-end distance R of the chain in a good solvent scale as $N\rho_a^{1/3}$, where N is the chain length and ρ_a is the grafting density. Since then there have been a large number of experimental, theoretical, and numerical studies of end-grafted polymer brushes. While most of the early studies were concerned with brushes in a good solvent, recently there has been considerable interest in understanding brushes in Θ and poor solvent conditions.

In a good solvent, self-consistent field (SCF) calculations,[5-12] which minimize the local free energy, found that h scaled as predicted by scaling theories and that the monomer density should decay as a parabola from its maximum value at the grafting surface to zero at h in the limit of long chains and strong overlap. For high coverages, higher order interactions become important and the density profiles are expected to become flatter than a parabola.[13,14] A mean field approximation in which a chain is in the mean field of the other chains and the solvent has also been developed.[15] Computer simulations[6,16-19] have confirmed these predictions and have given further details of the structure of the brush. Experimentally, the surface force apparatus,[20-23] small-angle neutron scattering,[24,25] and neutron reflectivity[26-29] have been very important in determining some of the properties of end-grafted polymeric brushes. The former gave the first direct measure of the brush height but not the density profile, which can be studied by the latter two methods. Both give results which are consistent with the SCF predictions.

The structure of a brush in a Θ or poor solvent has been the subject of several recent theoretical,[8,13,30-35] experimental,[25,29,36] and simulation studies.[37-39] At the Θ temperature, T_Θ, the brush height h is predicted to scale as $N\rho_a^{1/2}$ and the density profile should decay as an ellipse as long as binary interactions dominate.[32] To reach this regime, ρ_a must be larger than the overlap threshold ρ_a^*, which increases as the solvent quality decreases. However, as higher order interactions become important, the SCF theory can no longer be carried out analytically, and they must be evaluated numerically as done by Whitmore and Noolandi.[31] Recent Monte Carlo[37] and molecular dynamics[38] simulations confirmed the scaling of h but not the form of the density profile predicted by the analytic SCF theory. The reason for this lack of agreement is probably due to the fact that it was not possible to study long enough chains at low enough ρ_a to reach the regime where only binary interactions dominate. In most of the regime which is presently accessible to computer simulations, either the chains are not overlapping strongly enough or the overall monomer density is too large. Even for the longest chains studied in our previous simulations, $N = 200$, it was not possible to reach this regime. The simulation results are in qualitative agreement with the numerical SCF calculations[31] which showed that in a Θ solvent for degrees of polymerization appropriate for many experimental systems the monomer density $\rho(z)$ does not scale with z/N, where z is the distance from the grafting plane. This is clearly a minimum requirement for scaling theory to hold. This result indicates the difficulty in reaching the strongly overlapping regime without increasing the monomer density so much that the binary interactions no longer dominate. Mapping our simulation results[38] on coarse-grained brushes suggests that it will be very difficult to satisfy both the strong overlap and dominance of binary interactions implicit in the analytic SCF treatments for T near T_Θ.

In the poor solvent, SCF theory can be applied as long as the system remains homogeneous parallel to the grafting surface. In this regime, SCF predicts that the brush height

® Abstract published in *Advance ACS Abstracts*, December 15, 1993.

0024-9297/94/2227-0418$04.50/0

$h \sim N\rho_a$ and the density profile becomes more steplike as T is reduced. For high coverages and long chains, simulation results[37,38] confirm the predicted scaling behavior of h and the form of the density profiles. However, they also found an unexpected new phenomenon when the chains were not strongly overlapping. In this regime, the system phase separates into monomer-rich and monomer-poor regions. Because the chain ends are attached at one end to the surface and cannot move, this phase separation is local, not global. This phase separation, first observed by Lai and Binder,[37] has recently been explained within the random phase approximation by Yeung *et al.*[34] They found that for fixed N and ρ_a the grafted layer is unstable to tangential fluctuations in a sufficiently poor solvent. When the mean field solutions become unstable, the end-grafted polymers clump together to form a "dimpled" surface, in agreement with simulation results.[37,38] Huang and Balazs[35] found a similar effect using a two-dimensional numerical mean field model. Recently, Tang and Szleifer[40] have determined the phase diagram for grafted chains in a poor solvent using scaling arguments. They find the low-density mushroom regime, the uniform layered regime, and a microphase-separated or cluster regime, in agreement with the simulations. To observe this effect, the chains must be chemically adsorbed to the surface and the brush must be in equilibrium with a polymer-free solution. If both of these conditions are not satisfied, this local phase separation will not occur. If the brush is in equilibrium with chains in solution, then as the solvent quality is reduced some of the chains in solution will go the surface, producing a uniform surface profile. If there are no chains in solution but the chains are not strongly attached to a specific point on the surface, then the phase-separated regions can grow, albiet slowly, as a function of time.

Until now all but one simulation[41] of polymer brushes has been for chains grafted with infinite binding energy for fixed ρ_a. In these simulations, M chains of length N are attached randomly for a surface of area A at a fixed grafting density $\rho_a = M/A$. In this case, the effect of varying T or solvent quality is only to change the relative interaction of the monomers on the chains. While this is the dominant effect for polymers which are chemically attached to the surface or for diblock copolymers with long anchoring blocks, it is not always the case. There are at least two other interesting cases. One is when the polymers are end grafted with only a moderate binding energy, and another is when the adsorbing block is free to adjust to an external pressure, as for a diblock copolymer in a selective solvent in which one of the blocks is submerged and the other spreads at the interface. In the former, changing either N or T also changes ρ_a. For the case of polystyrene (PS) end functionalized with a zwitterion, the binding energy is only of order $(6\text{–}8)k_BT$, and ρ_a is observed to depend significantly on the chain length, $\rho_a \sim N^{-2\nu}$ in a good solvent ($\nu = 0.59$). This effect can be explained[20] by noting that each k_BT of binding energy can support about one blob. The larger N, the larger each blob will be, resulting in a lower coverage. Perahia *et al.*[29] observed similar effects as the solvent quality was varied using neutron reflectivity. In the vicinity of the Θ point, ρ_a was found to increase in such a way that the height h remained nearly constant as the solvent quality decreased. The coverage can also be changed by applying an external surface pressure Π_a to a diblock copolymer at a liquid–air interface. A monolayer of poly(dimethylsiloxane)–polystyrene (PDMS–PS) diblock copolymers at the surface of a selective solvent, such as tricresyl phosphate[42] or ethyl benzoate,[27,28] is an example of such a system. The PS block is submerged in the liquid, while the PDMS block spreads as a monolayer at the air surface. When the length of the PS block is much longer than the PDMS block, the external applied surface pressure is balanced predominantly by the interactions of the PS monomers. In this case, the results can be compared directly with the theoretical results on end-grafted brushes. To simulate either case, one must take an approach different from that used in the past. In the former case, one might try to simulate end-grafted polymers with a finite binding energy in equilibrium with a low density of polymers in solution. However, due to the very slow equilibration times, this is only possible for very short chains.[41] Simulations in the latter case, namely, when Π_a and not ρ_a is constant, are more straightforward and are presented here. The results of these simulations can be compared directly to the recent neutron reflectivity studies of Kent *et al.*[27] on diblock copolymers at an air–liquid interface and also used as a further test of the SCF theory, which has a prediction for the scaling form of Π_a as a function of N and ρ_a for different solvent qualities. An additional advantage of the constant-pressure simulations is that ρ_a can be changed dynamically by simply varying Π_a, allowing us to study a wider range of ρ_a than in previous simulations.

The osmotic pressure Π for a bulk solution of density ρ is given by[43]

$$\Pi = -\frac{\partial(f/\rho)}{(1/\rho)} = \rho^2\frac{\partial(f/\rho)}{\partial\rho} \tag{1}$$

where f is the free energy per unit volume. In a brush, even though the monomer density $\rho(z)$ and osmotic pressure $\Pi(z)$ depend on the distance z from the grafting surface, eq 1 should still be true. From $\Pi(z)$, which has not been examined in previous simulations, and $\rho(z)$, the equation of state for monomers in the brush can be determined. For sufficiently large chain length N and all grafting densities ρ_a, $\Pi(z)$ versus $\rho(z)$ collapsed onto a single curve which could be fit reasonably well by the Flory–Huggins formula. The surface osmotic pressure Π_a is related to the change of free energy per unit surface area,

$$\Pi_a = -\partial f_c/(\partial\rho_a^{-1}) \tag{2}$$

where f_c is the free energy per chain. In the scaling theory of Alexander,[3] each chain consists of N/g blobs stretching away from the surface, where g is the number of monomers in each blob. In a good solvent, the blob size equals the mean interanchor spacing $s = g^{3/5}a$, where a is the monomer size. Since the excess repulsive energy per blob is about k_BT, the excess repulsive energy per chain is of order $(N/g)k_BT$. Since $\rho_a \sim s^{-2}$, the free energy per chain $f_c \sim N\rho_a^{5/6}k_BT$ and the surface pressure $\Pi_a \sim N\rho_a^{11/6}k_BT$. In mean field theory,[1] in which one uses a Flory-type argument to balance the stretching energy and the excluded volume energy, one obtains a slightly different result, namely, $\Pi_a \sim N\rho_a^{5/3}$. While both theories give the same result for h, the difference in f and Π_a reflects the fact that the mean field ansatz overestimates both the repulsive and attractive terms in the free energy in the same way. In a Θ solvent, both theories predict that $\Pi_a \sim N\rho_a^2$. The present simulations, however, do not agree with either of these predictions. Instead the simulations give a stronger dependence on ρ_a, namely, $\Pi_a \sim N\rho_a^x$ with $x = 2.5 \pm 0.2$ in a good solvent and $x = 3.0 \pm 0.2$ in a Θ solvent. These results are, however, consistent with the statistical thermodynamic theory of grafted polymers developed recently by Carignano and Szleifer.[15] They[44] found that $x \approx 2.4$ in a good solvent and 3.0 in a Θ solvent.

The origin of this difference with the mean field and scaling theories is not presently understood.

In the next section, I describe the model and the constant-pressure molecular dynamics method used in this study. In section III, I describe the results for the coverage ρ_a and brush height h as a function of osmotic pressure Π_a and solvent quality. Results are compared to SCF theory. In section IV, results for the monomer density profile $\rho(z)$ and the osmotic pressure profile $\Pi(z)$ will be presented. Effects of a small attractive interaction between the grafting surface and the monomers are also included. A brief summary is presented in section V.

II. Model and Method

The equilibrium structure of the brush was obtained using a constant surface pressure molecular dynamics method in which each monomer is coupled to a heat bath. The system consists of M polymers of $N + 1$ monomers attached to the $z = 0$ plane. Periodic boundary conditions are used in the x and y directions. The interaction potential U_i is composed of three terms: $U_i = U^0 + U^{ch} + U^w$.[38] U^0 is the standard 6–12 Lennard-Jones interaction truncated at $r_c = 2.5\sigma$, where σ is the Lennard-Jones unit of length. By extending the range of the interaction to 2.5σ, the effects of solvent quality can be introduced by simply varying the temperature T, without having to explicitly introduce solvent particles. The second interaction U^{ch} is an attractive potential binding the monomers along the chain.[38] In order to maintain an average bond length which is essentially independent of T, the strength of U^{ch} depended linearly on T. The third interaction is the wall–monomer interaction. In our earlier simulations,[16] we used a purely repulsive interaction between the monomers and the grafting surface (wall). However, to allow for attractive wall–monomer interactions, we[38] replaced the original purely repulsive interaction with a long-range attractive interaction of the form

$$U^{aw} = 4\pi\bar{\rho}\epsilon^{aw}\left[\frac{1}{5}\left(\frac{\sigma}{z-\sigma/2}\right)^{10} - \frac{1}{2}\left(\frac{\sigma}{z-\sigma/2}\right)^{4}\right] \qquad (3)$$

where ϵ^{aw} is the interaction strength. This form of the interaction arises from assuming a Lennard-Jones interaction between the monomers and the surface atoms and integrating over the xy plane. In the present simulations, we took the density of surface atoms $\bar{\rho} = 0.80$ and varied ϵ^{aw}. For small $\epsilon^{aw} \approx 0.1\epsilon$, the repulsive part of U^{aw} dominates and the results are identical to those using our original, purely repulsive potential.[38] Unless otherwise specified, all of the simulations presented here are for $\epsilon^{aw} = 0.1\epsilon$, where ϵ is the strength of the Lennard-Jones interaction which acts between any two monomers. In section IV, some results are presented for $\epsilon^{aw} = \epsilon$, since these agree better with the density profiles determined from neutron reflectivity experiments by Perahia *et al.*[29] for PS end grafted onto silicon which show a small surface excess.

In contrast to our previous studies, the surface osmotic pressure, Π_a, is fixed instead of ρ_a. This is done following the method developed by Andersen[45] and Parrinello and Rahman.[46] Andersen originally proposed a method for constant-pressure molecular dynamics in three dimensions in which the system is coupled to the volume of the simulation cell through the action of a piston. Parrinello and Rahman generalized this method to allow for the simulation cell to change shape as well as size. Since the simulation cell is periodic in two directions and open in the third, a method similar to that of Parrinello and Rahman was applied, except that the surface area of the cell was allowed to change size but the shape of the cell was kept rectangular. This is done by introducing two extra equations of motion to describe the motion of the length L_x and L_y of the simulation cell in addition to the equations of motion for the MN monomers. The applied pressure Π_a is balanced by the internal osmotic pressure $\mathcal{P}_\alpha$ in the $\alpha = x$ and y directions,

$$\mathcal{P}_\alpha A = \sum_i m\dot{r}_{i\alpha}^2 + \sum_i \sum_{j>i} r_{ij\alpha} f_{ij\alpha} \qquad (4)$$

Here m is the monomer mass, $r_{i\alpha}$ is the α coordinate of particle i, $r_{ij\alpha} = r_{i\alpha} - r_{j\alpha}$, and $f_{ij\alpha}$ is the force between monomers i and j. The "potential energy" associated with the surface area is $\Pi_a A$, and the extra kinetic energy is

$$\mathcal{K}_A = \frac{1}{2} M_w \sum_{\alpha=1}^{2} \dot{L}_\alpha^2 \qquad (5)$$

where M_w is the wall mass. In the early runs, I used this method. However, in some cases, the lengths of the cell, L_x or L_y, drifted apart, until one of them was significantly smaller than the other. When this happened, the run had to be stopped and restarted. To avoid this problem, in later runs, the average osmotic pressure $\bar{\mathcal{P}} = (\mathcal{P}_1 + \mathcal{P}_2)/2$ was applied in both directions so that the simulation cell remained square. Results from both methods gave similar results. It is important to note that Π_a can also be determined in a constant ρ_a simulation, though this has not been done in any previous simulation. Results for constant Π_a and constant ρ_a simulations gave the same results. Further details on the simulation technique can be found elsewhere.[38]

The equations of motions[47] are integrated using a velocity–Verlet algorithm with a time step Δt, taken to be as large as possible, while keeping the integration stable. I used 0.006–0.008τ in the present simulations, where $\tau = \sigma(m/\epsilon)^{1/2}$. The higher T is, the smaller the time step. The mass of the wall M_w was taken to be between m and $20m$ and the friction coefficient $\Gamma = 0.5\tau^{-1}$. In the rest of the paper, I use units in which $m = \sigma = 1$. The temperature T is measured in units of ϵ/k_B, the coverage ρ_a in units of σ^{-2}, the surface pressure Π_a in units of ϵ/σ^2, and osmotic pressure $\Pi(z)$ in units of ϵ/σ^3. In a previous simulation on a single chain,[38] the Θ temperature was found to be $T_\theta = 3.0 \pm 0.1$.

Using this method, I simulated brushes consisting of $N + 1$ monomers, with N between 25 and 200 for a range of surface pressures Π_a. In most of the runs, the first monomer is firmly attached to a specific site on the grafting surface, which is located on the xy plane. However, in some runs, the grafted end is annealed, in that it is allowed to move within the grafting plane. For all cases, $M = 50$ chains were randomly attached to the surface. This was a large enough number to ensure that the chains do not cross the periodic boundaries more than once in either direction. The simulations were started by growing random walk chains starting from the grafting site on the wall with a bond length of σ and a restriction to avoid backfolding.[48] This was done by simply requiring that $|\mathbf{r}_{i-1} - \mathbf{r}_{i+1}| > \sigma/4$ where r_0 is of order σ. To remove the overlap, a softer potential[48] which does not diverge at short distance is used for a few thousand steps. To check that the systems were equilibrated, several states were initiated from one with a lower Π_a (lower ρ_a) or a higher Π_a (higher ρ_a). Both gave the same result within statistical error. After long equilibration runs (typically $(3$–$10) \times 10^4\Delta t$), the simulations were run between $6 \times 10^4\Delta t$ and $30 \times 10^4\Delta t$. For further analysis, the monomer coordinates were saved every 1000–2000 steps. Several quantities were

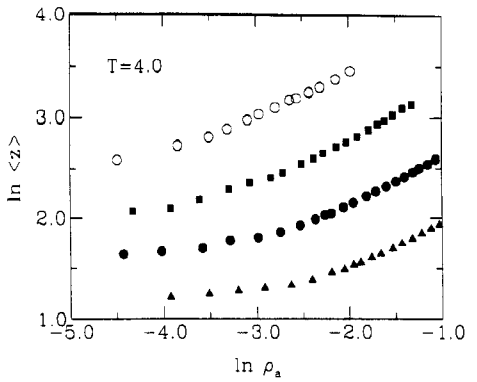

Figure 1. Average monomer height $\langle z \rangle$ versus grafting density ρ_a in a good solvent at $T = 4.0$ for chain lengths $N = 25$ (▲), 50 (●), 100 (■), and 200 (○). The wall–monomer interaction $\epsilon^{aw} = 0.1\epsilon$ and the grafting sites are fixed.

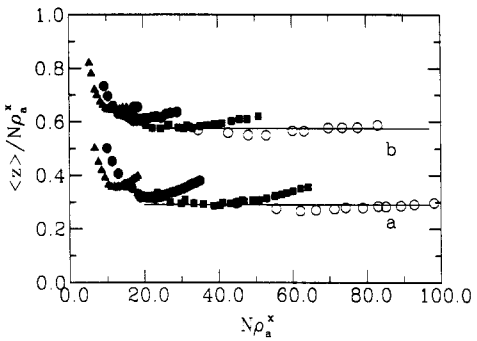

Figure 2. Average monomer height $\langle z \rangle$ versus $N\rho_a^x$ for brushes in a good solvent at $T = 4.0$, $x = 1/3$ (a) and at the Θ temperature $T = T_\Theta = 3.0$, $x = 1/2$ (b). The results for $T = 3.0$ have been shifted vertically by 10 for clarity. The data are from the constant Π_a runs presented here as well as from the constant ρ_a runs of ref 38. The wall–monomer interaction $\epsilon^{aw} = 0.1\epsilon$ and data are for chains with a fixed grafting site and for annealed chains in which the chain end is free to move within the grafting plane.

calculated from these configurations, including the local monomer density $\rho(z)$ and the local monomer osmotic pressure $\Pi(z)$. The integral of $\Pi(z)$ is the total pressure Π_a. The brush height h can be determined from either h_{max}, the point where $\rho(z)$ extrapolates to zero, or $\langle z \rangle$, the first moment of $\rho(z)$. Because of rounding of the $\rho(z)$ due to finite chain lengths N, h_{max} is more uncertain than $\langle z \rangle$, though both contain the same information. Results for other quantities, like the density of free ends of the chain $\rho_E(z)$, the mean square end-to-end distance, and the mean squared radius of gyration of the chains, have already been discussed elsewhere.[38] Results for all of these quantities are consistent with those reported previously.

III. Results

Good Solvent Conditions. The brush height h has been shown previously to have the expected scaling with N and ρ_a, $\langle z \rangle \sim N\rho_a^{1/3}$ in a good solvent provided that ρ_a was greater than the overlap coverage $\rho_a^* \sim N^{-6/5}$. Results from the present simulations are shown in Figure 1 for $25 \leq N < 200$ and a wide range of coverages, $0.01 < \rho_a < 0.40$. The uncertainty in the data is about 3–4%. In Figure 2, a scaling plot of $\langle z \rangle / N\rho_a^{1/3}$ is presented as a function of the scaling variable $N\rho_a^{1/3}$ for a good solvent (curve a). Data are from the present constant Π_a simulations as well as from our earlier simulations[38] at constant ρ_a. For low coverages h is nearly independent of ρ_a, as expected in the mushroom regime below ρ_a^*. For low coverages h is nearly independent of ρ_a, as expected in the mushroom regime below ρ_a^*. For $\Pi_a = 0$, the surface area increases so that chains are no longer in contact as expected. As seen in Figure 2, $\langle z \rangle$ follows the expected scaling behavior for $\rho_a > \rho_a^*$ with both N and ρ_a provided ρ_a is not too large. At ρ_a^*, the brush is moderately stretched, $h_{max}/\langle R_G^2 \rangle^{1/2} \sim 4$ and $\pi\langle R_G^2 \rangle \rho_a \sim 2.3$, where $\langle R_G^2 \rangle$ is the mean squared radius of gyration of a free polymer in dilute solution at the same T. For the longest chains and highest coverages studied, $h_{max}/\langle R_G^2 \rangle^{1/2} \sim 9$ and $\pi\langle R_G^2 \rangle \rho_a \sim 30$. Since $\rho_a^* \sim N^{-6/5}$, the scaling variable evaluated at the lower crossover, $N\rho_a^{*1/3} \sim N^{3/5}$, is not universal but increases with N, in agreement with the results shown in Figure 2. For $\rho_a > \rho_{a1} \approx 0.12$, $\langle z \rangle$ increases faster than $\rho_a^{1/3}$, accounting for the deviations in the scaling plot for $\langle z \rangle / N\rho_a^{1/3}$. In this regime, the average monomer density ρ is greater than 0.45, which is more than half of the melt density for this model. In this regime as seen from Figure 1, h scales as ρ_a^x, with x approximately equal to $1/2$, in agreement with Raphaël, Pincus, and Fredrickson,[49] who showed that when three-body terms dominate over two-body terms there is a second scaling regime with $x = 1/2$ instead of $1/3$. Note that experimentally it is difficult to reach such high coverages in order to study this regime. The limited scaling regime, $\rho_a^* < \rho_a < \rho_{a1}$ where $\langle z \rangle \sim N\rho_a^{1/3}$, also makes it difficult to test the dependence of h on ρ_a experimentally.[28] If the chains are not long enough, $\rho_a^* \sim \rho_{a1}$ and there is no regime in which the data scale as predicted theoretically, as seen for $N = 25$. For intermediate length chains, the scaling regime is very limited, as for $N = 50$. For $N = 50$ and 100, h scales almost linearly with ρ_a for a wide range of ρ_a from the mushroom regime to $\rho_a \approx 0.30$ ($\pi\langle R_G^2 \rangle \rho_a \approx 16$) and 0.11 ($\pi\langle R_G^2 \rangle \rho_a \approx 12$), respectively. This may explain the data of Factor *et al.*[28] for PS in a good solvent for molecular weight up to 175 000, who found that h varied approximately linearly with ρ_a over the entire range studied, $\pi\langle R_G^2 \rangle \rho_a < 11$. Only for long chains is ρ_a^* significantly less than ρ_{a1} and the scaling prediction valid over an extended range.

In Figure 3, results for the surface pressure Π_a as a function of ρ_a are shown for four values of the chain length N in a good solvent. Note that as the chain length increases, the surface pressure Π_a increases very rapidly with ρ_a. As seen from Figure 3b, for $\rho_a \gtrsim 0.05$, $\Pi_a \sim \rho_a^y$, with $y = 2.5 \pm 0.2$. In the regime $\rho_a^* < \rho_a < \rho_{a1}$ where $h \sim N\rho_a^{1/3}$, y may be slightly smaller, 2.3 ± 0.2, but this regime is very limited. In either case, this result for y is in contrast with SCF mean field theory, which predicts that $\Pi_a \sim \rho_a^{5/3}$, and scaling theory, which suggests a slightly different power law, $\Pi_a \sim \rho_a^{11/6}$. A scaling plot for $\Pi_a / N\rho_a^{5/3}$ versus ρ_a is shown in Figure 4. Note that even for $\rho_a^* < \rho_a < \rho_{a1}$, where $\langle z \rangle$ scales as predicted, the surface osmotic pressure Π_a increases more rapidly than predicted. For $\rho_a > \rho_{a1}$, the data also show a weak systematic dependence on N, as the results for $\Pi_a / N\rho_a^{5/3}$ increase slightly with N for fixed ρ_a. The observed value for the exponent y is not understood theoretically. While it may be the result of a breakdown of the theories, a more likely explanation is that Π_a is more sensitive to the finite monomer density than the brush height. For the range of N and ρ_a studied, $\rho(z)$ in the center of the brush is at least 0.12 for even the lowest ρ_a studied. This gives rise to a purely steric effect which limits the interpenetration of the chains but which is not included in either the scaling or SCF theories. This extra contribution to Π_a may account for the stronger dependence of Π_a on ρ_a than predicted. However, as seen in Figure 2, this finite volume fraction does not affect h as much. As a check on this idea, one can compare Π_a from the simulations with the scaling prediction, $Th\rho_a^{3/2}$, which should be correct within prefactors of order unity. Using $\langle z \rangle$ as a measure of h, Π_a

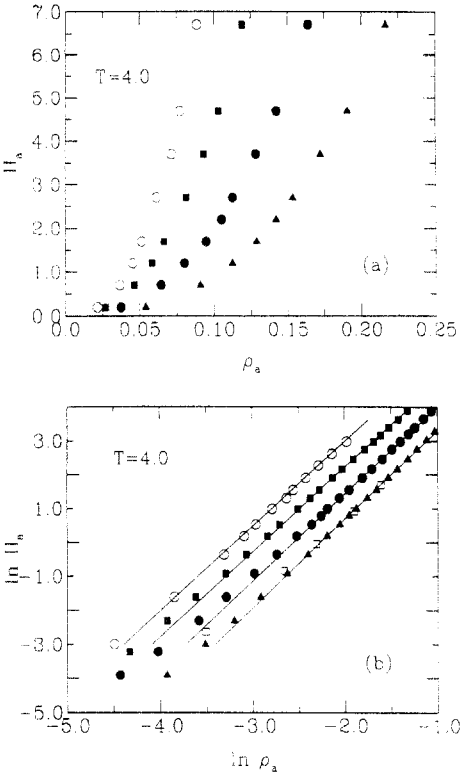

Figure 3. Surface pressure Π_a versus grafting density ρ_a in a good solvent at $T = 4.0$ for chain lengths $N = 25$ (▲), 50 (●), 100 (■), and 200 (○). The wall–monomer interaction $\epsilon^{aw} = 0.1\epsilon$ and the grafting sites are fixed. The slopes of the lines drawn through the data for large ρ_a in (b) are $y = 2.62$ for $N = 25$, 2.57 for $N = 50$, and 2.50 for $N = 100$ and 200. The open squares are the results of Carignano and Szleifer[15] for chain length $N = 50$ in a good solvent.

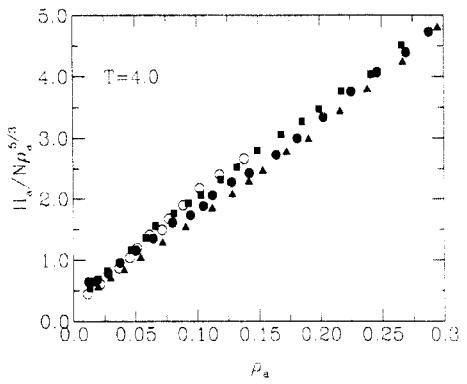

Figure 4. Scaling plot of $\Pi_a/N\rho_a^{5/3}$ versus ρ_a in a good solvent at $T = 4.0$. Symbols are the same as in Figure 3.

as measured in the simulations equals the theoretical SCF result $T\langle z\rangle\rho_a^{3/2}$ for $\Pi_a \simeq 0.2$ for all four values of N. For most of the accessible range, the measured Π_a is significantly larger than $T\langle z\rangle\rho_a^{3/2}$. Thus one possible explanation of these results is that Π_a only scales for $\Pi_a \lesssim 0.2$ and $\rho(z) \lesssim 0.10$. However, this regime is well beyond the range of the present simulations and would require $N \sim 1000$ since even for $N = 200$ the brush is only weakly stretched for such low ρ_a. This also appears to be a very difficult regime to access experimentally as well.

While these results do not agree with the SCF and scaling theories, they do agree with the recent experimental results of Kent *et al.*[27,50] and with the theoretical results of Carignano and Szleifer.[15] Kent *et al.* found that for PDMS–PS diblock copolymers in a selective solvent (ethyl benzoate) the surface pressure increased more rapidly than predicted by the scaling and SCF theories. Their results are in qualitative agreement with Figure 3a. Carignano

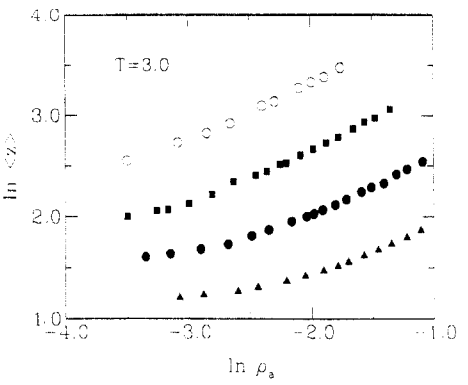

Figure 5. Average monomer height $\langle z\rangle$ versus ρ_a in a Θ solvent at $T = T_\Theta = 3.0$ for chain lengths $N = 25$ (▲), 50 (●), 100 (■), and 200 (○). The wall–monomer interaction $\epsilon^{aw} = 0.1\epsilon$ and the grafting sites are fixed.

and Szleifer[15] developed a statistical thermodynamic in which one considers a chain in a mean field of the other chains and the solvent. In this approach, the finite volume of the segments and the solvent is explicitly included. The pressure has two contributions, one from the pure chain–chain interaction and the second from the change in the composition of the solvent throughout the layer which occurs when the area is changed. This solvent contribution is not explicitly taken into account because in those theories the solvent is only included at the level of the second virial coefficient. They[44] find that Π_a increases approximately as ρ_a^y with $y \approx 2.4$. In fact, as seen in Figure 3b, their data for $N = 50$ are nearly on top of our results.

Θ Solvent Conditions. At the Θ temperature T_Θ, the brush height is expected to scale as $N\rho_a^{1/2}$. This result was confirmed in earlier simulations by Lai and Binder[37] and Grest and Murat.[38] Results from the present simulations for fixed chain ends are shown in Figure 5 for a wider range of ρ_a. As in the good solvent case, we see that for low ρ_a h increases very slowly with ρ_a. This corresponds to the mushroom regime where the chains are not strongly overlapping. A scaling plot of $\langle z\rangle/N\rho_a^{1/2}$ is shown in Figure 2 (curve b). Note that chains of length = 25 and 50 are too short to reach the scaling regime, while data for $N = 100$ and 200 are clearly in the scaling regime for intermediate ρ_a. At ρ_a^*, $h_{max}/\langle R_G^2\rangle^{1/2} \sim 4$ and reaches a value of about 9 for large ρ_a and N. For $\rho_a \gtrsim 0.13$, the height increases slightly faster than $\rho_a^{1/2}$ (approximately as $\rho_a^{0.58\pm0.02}$) and h deviates from the scaling prediction.

The surface pressure Π_a is expected to scale as $N\rho_a^2$ at the Θ temperature from both scaling and SCF theories. However, as observed in the good solvent case, a stronger dependence on the grafting density is found, $\Pi_a \sim \rho_a^y$, where $y = 3.0 \pm 0.2$, as seen in Figure 6. In the mushroom regime, at small Π_a, the results deviate from the apparent power law dependence as expected. A scaling plot of $\Pi_a/N\rho_a^2$ is shown in Figure 7. Note that the data do not collapse as well as in a good solvent, in part because of a weak dependence of y on N. The value of 3.0 agrees with that found by Carignano and Szleifer[44] for a Θ solvent using their statistical thermodynamic model.

Effect of Annealing. In many experiments on polymer brushes as well as most previous simulations, the chain ends are fixed to a specific point on the surface. However, in some experiments, such as in the case of diblock copolymer at a selective solvent, the chain ends are free to move as long as they remain at or very near the interface. To examine the effect of allowing the ends to move, additional simulations were carried out in which the chain end was free within the grafting plane. For a fixed ρ_a, results for the monomer density $\rho(z)$ and $\langle z\rangle$ were the

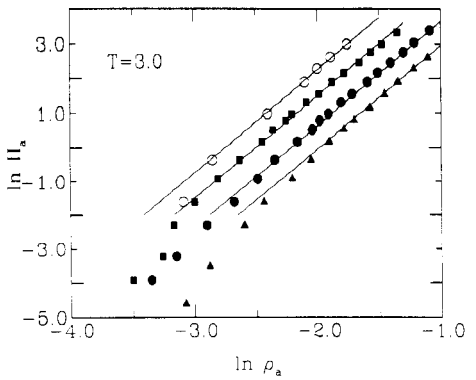

Figure 6. Surface pressure Π_a versus ρ_a in a Θ solvent (T = 3.0) for chain lengths N = 25 (▲), 50 (●), 100 (■), and 200 (○). The wall–monomer interaction $\epsilon^{aw} = 0.1\epsilon$ and the grafting sites are fixed. The slope of the lines is y = 3.0 for all four cases for large ρ_a.

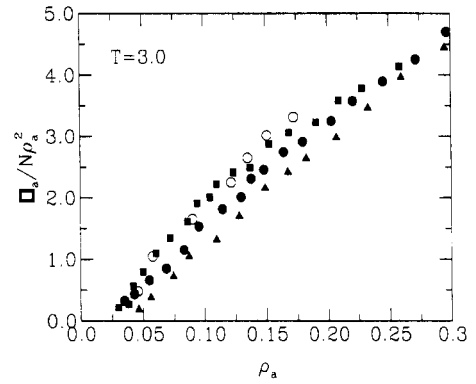

Figure 7. Scaling plot of $\Pi_a/N\,\rho_a^2$ versus ρ_a in a Θ solvent (T = 3.0). Symbols are the same as in Figure 6.

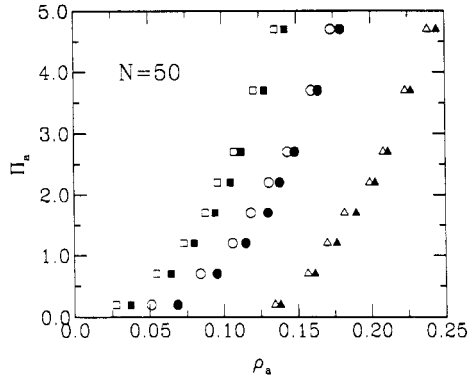

Figure 8. Surface pressure Π_a versus grafting density ρ_a for chain length N = 50 in a good solvent at T = 4.0 (squares), in a Θ solvent, $T = T_\Theta$ = 3.0 (circles), and in a poor solvent at T = 2.0 (triangles). The closed symbols are for the case when the grafting sites are fixed, while the open symbols are for annealed chains in which the chain end is free to move within the grafting plane.

same for annealed and fixed chain ends. Results for $\langle z \rangle$ for the annealed case have been included in the scaling plot for $\langle z \rangle$ (Figure 2). The only difference between these two cases is in the grafting density for a given surface pressure as seen in Figure 8, where Π_a versus ρ_a is shown for N = 50 for three temperatures. Here results for both fixed grafted sites (closed symbols) and annealed chains (open symbols) are shown. The small difference in the two cases comes from the additional force between the grafting site and the first mobile monomer. For chains grafted to a specific site, there is an additional contribution to Π_a. In the annealed case, the monomers near the grafted end of the chain have more degrees of freedom, causing a lower mean ρ_a compared to the fixed grafted site case.

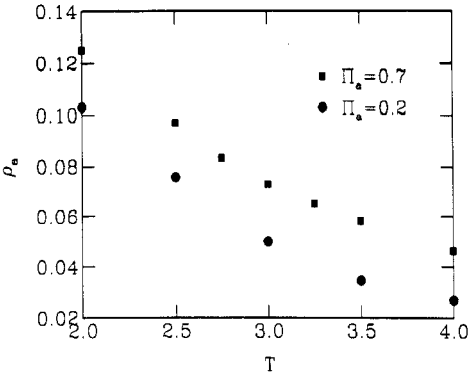

Figure 9. Grafting density ρ_a versus temperature T for chains of length N = 100 for two values of the surface pressure Π_a. The grafting sites are fixed.

For fixed Π_a, the difference in ρ_a between the fixed and annealed grafting sites decreased as N^{-1} as expected for an end effect. For the annealed case for low ρ_a, Π_a goes to the ideal gas law, $k_BT\rho_a$, while for the fixed grafted site case, $\Pi_a < k_BT\rho_a$ due to the extra contribution from fixing the grafting site.

Results for ρ_a versus T are shown in Figure 9 for two values of Π_a for N = 100. Note that ρ_a varies smoothly as the solvent quality is decreased. Because these simulations were carried out at constant surface pressure, there is no two-phase coexistence regime at low T in contrast to the micro phase separation observed for constant-coverage simulations by Lai and Binder[37] and Grest and Murat.[38] For fixed Π_a, ρ_a increases continuously as T is decreased. While these results are consistent with a number of theoretical SCF calculations[13,30,32,33] that suggested that changing the solvent quality causes the brush to collapse continuously and uniformly, it should be noted that these studies did not allow for the possibility that the grafted layer may become unstable to tangential fluctuations in a sufficiently poor solvent. For fixed ρ_a, when these fluctuations become sufficiently strong, the uniform brush is unstable and the system phase separates[34,35] into monomer-rich and monomer-poor regimes. However, at constant Π_a, this two-phase coexistence regime does not exist and the transition is continuous.

IV. Structure of the Brush

The structure of the brush has been studied in detail in a number of previous publications for good, Θ, and poor solvents. All of these studies have concentrated on the scaling of the monomer number density $\rho(z)$ with z/N and how $\rho(z)$ changes shape as ρ_a is varied. For a good solvent, these simulations have given convincing evidence that $\rho(z)$ is a parabola for an intermediate range of coverages and that these profiles become flatter than a parabola for larger ρ_a. However, in none of these previous simulations was the osmotic pressure $\Pi(z)$ measured.

The dependence of the monomer density is shown as a function of the distance from the grafting surface in Figures 10 and 11 for Π_a = 0.2 and 0.7 for three values of T. Results are for chains grafted to a fixed grafting site. The results in Figure 10 are for a wall–monomer interaction $\epsilon^{aw} = 0.1\epsilon$, which can be thought of as purely repulsive for these temperatures. Figure 11 presents results for $\epsilon^{aw} = \epsilon$, which has an excess monomer density near the wall. The feet in $\rho(z)$ for z near h_{max} are caused by fluctuations of the average trajectory of the chains near the ends where the chain stretching is weak. This rounding of the profile goes away as N increases.[10,12,38] Note that as the quality of the solvent decreases, the shape of the profile changes

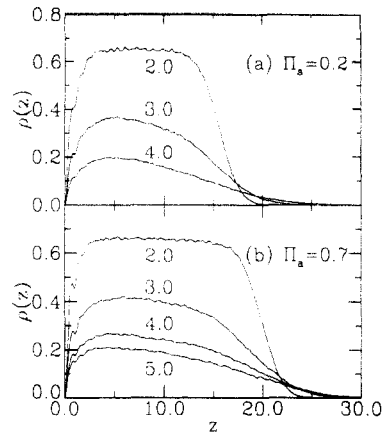

Figure 10. Monomer number density $\rho(z)$ as a function of the distance from the grafting surface for chains of length $N = 100$ at $T = 2.0$, 3.0, and 4.0 for two values of the surface pressure Π_a. The wall–monomer interaction strength $\epsilon^{aw} = 0.1\epsilon$ and the grafting sites are fixed. For $\Pi_a = 0.2$, $\rho_a = 0.27$ ($T = 4.0$), 0.050 ($T = 3.0$), and 0.103 ($T = 2.0$). For $\Pi_a = 0.7$, $\rho_a = 0.036$ ($T = 5.0$), 0.047 ($T = 4.0$), 0.072 ($T = 3.0$), and 0.129 ($T = 2.0$).

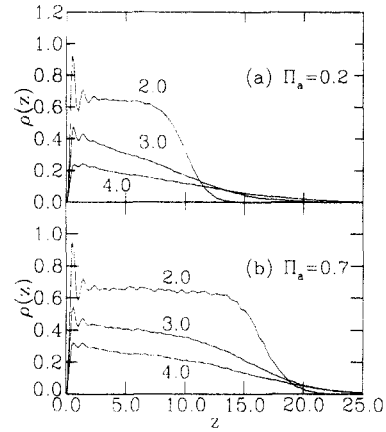

Figure 11. Monomer number density, $\rho(z)$, as a function of the distance from the grafting surface z for $N = 100$. This figure is similar to Figure 10, except that the wall–monomer interaction strength has been increased to $\epsilon^{aw} = \epsilon$. Note the increase of the density of monomers near the surface as ϵ^{aw} increases. For $\Pi_a = 0.2$, $\rho_a = 0.024$ ($T = 4.0$), 0.036 ($T = 3.0$), and 0.063 ($T = 2.0$). For $\Pi_a = 0.7$, $\rho_a = 0.040$ ($T = 4.0$), 0.063 ($T = 3.0$), and 0.107 ($T = 2.0$).

as expected. In the good solvent ($T = 4.0$), these profiles have a parabolic shape and cross over smoothly to a more steplike shape as the solvent quality decreases. However, as T decreases, ρ_a increases (see Figure 5) in such a way that the height remains essentially constant. Results for $\langle z \rangle$, which is a better measure of the height than h_{max}, are the same within our statistical error for the data shown in Figures 10 and 11b. Only for very low $\Pi_a \approx 0.2$ and strong wall–monomer interaction, $\epsilon^{aw} = \epsilon$, as shown in Figure 11a, did the height of the brush decrease as T decreased. However, even for this relatively strong wall–monomer interaction, for a slightly larger value of $\Pi_a = 0.7$, h is nearly independent of T as seen in Figure 11b. For very large values of Π_a and ρ_a, the height was observed to increase slightly, by about 6–8% as T decreased from 4.0 to 2.0. However, in these cases, $\rho_a \gtrsim 0.2$ and steric effects are important. Thus it appears that unless there are strong attractive wall–monomer interactions, the height should not change as the solvent quality is decreased. This finding can be tested by studying diblock copolymers at the liquid–air interface.

This result can be compared to the neutron reflectivity results of Perahia *et al.*[29] on end-functionalized PS grafted on silicon. In this case the polymer brush is in equilibrium

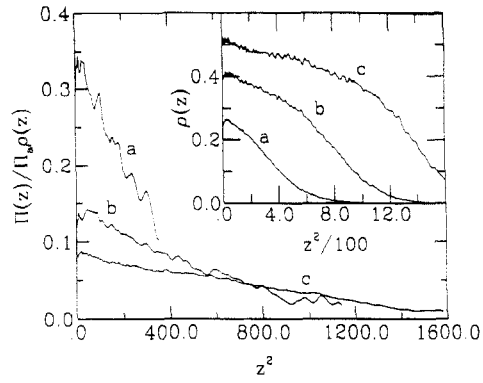

Figure 12. Osmotic pressure, $\Pi(z)/\Pi_a\rho(z)$, as a function of the distance from the grafting surface z for a good solvent for $T = 4.0$ and $N = 100$: (a) $\Pi_a = 0.7$, $\rho_a = 0.047$; (b) $\Pi_a = 4.7$, $\rho_a = 0.103$; (c) $\Pi_a = 15.7$, $\rho_a = 0.168$. The inset shows the monomer density $\rho(z)$ for the same three cases.

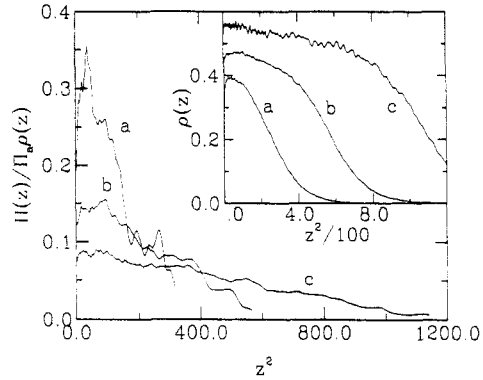

Figure 13. Osmotic pressure, $\Pi(z)/\Pi_a\rho(z)$, as a function of the distance from the grafting surface z for a Θ solvent ($T = 3.0$) for $N = 100$: (a) $\Pi_a = 0.4$, $\rho_a = 0.060$; (b) $\Pi_a = 2.2$, $\rho_a = 0.103$; (c) $\Pi_a = 8.7$, $\rho_a = 0.169$. The inset shows the monomer density $\rho(z)$ for the same three cases.

with a solvent containing a finite fraction of functionalized PS. They found that as the solvent quality was decreased in the vicinity of T_Θ, ρ_a increased in such a way that h remained essentially unchanged. Since the binding energy in this system is only $(6–8)k_BT$, chains go on and off the silicon surface and equilibrium is obtained when the chemical potential of the brush equals that of the solution. This equilibrium is determined by a balance between the stretching energy and the binding energy. Perahia *et al.*[29] use Flory theory to show that in the vicinity of T_Θ, the temperature dependence of h is much weaker than ρ_a. While their situation is different from that of the present simulations, in which Π_a is fixed, it is interesting that both give a brush height which is nearly independent of solvent quality. The agreement suggests that experimentally, the surface osmotic pressure is probably approximately constant as the solvent quality is varied. However, there is no argument that I am aware of which would suggest that equal chemical potential for the brush and solvent would lead to a constant or nearly constant surface osmotic pressure.

The dependence of the osmotic pressure, $\Pi(z)$, on the distance z from the grafting plane is also of interest since it can be used to check some of the assumptions in the SCF theory. $\Pi(z)$ is measured from the virial theorem and averaged over all monomers between $z - 0.1\sigma$ and $z + 0.1\sigma$ from the grafting plane. $\Pi(z)$ is also related to Π_a, $\Pi_a = \int_0^\infty \Pi(z)\,dz$. Results for $\Pi(z)/\rho(z)$ versus z^2 are shown for chains of length $N = 100$ for several values of ρ_a for a good and Θ solvent in Figures 12 and 13, respectively. The insets of the figures give the monomer density profiles $\rho(z)$ for the corresponding grafting densities. Note that

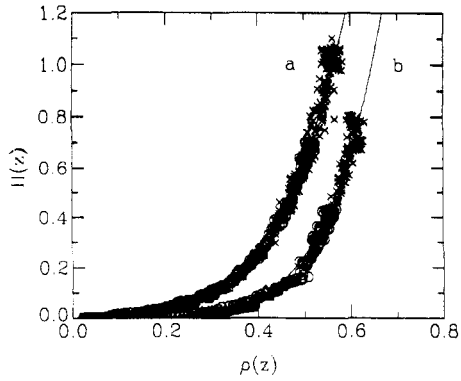

Figure 14. Surface pressure, $\Pi(z)$, versus $\rho(z)$ for (a) $T = 4.0$ and (b) $T = T_\Theta = 3.0$ for $N = 100$. For $T = 4.0$ the data are for four grafting densities ranging from $\rho_a = 0.047$ to 0.218. For $T = T_\Theta = 3.0$, data are for grafting densities ranging from $\rho_a = 0.060$ to 0.228.

$\Pi(z)/\rho(z)$ is approximately parabolic, even for large ρ_a where $\rho(z)$ is not. The scaling and SCF theories also suggest that the equation of state for a monomer at height z from the grafting density should depend only the local density, not on ρ_a or N, provided N is sufficiently large. In Figure 14, $\Pi(z)$ versus $\rho(z)$ is shown for $N = 100$ for $T = 3.0$ and 4.0 for several ρ_a. Similar results were obtained for $N = 50$. As expected, the results fall on one curve independent of ρ_a. Results for the bulk osmotic pressure Π of a three-dimensional melt of 50 chains of length $N = 100$ agreed with this equation of state for high densities but gave slightly lower values for Π than that shown in Figure 14 for low and moderate densities. For $\rho = 0.40$, the difference was about 15%, which may be due to end effects. These data can be fit reasonably well to the Flory–Huggins form,[43]

$$\Pi(z)/T = \Phi/N - \ln(1 - \Phi) - \Phi - \chi\Phi^2 \qquad (6)$$

where $\Phi = \rho(z)/\rho^*$ is the fraction of sites occupied. The solid lines in Figure 14 are fits to eq 6 with $\rho^* = 0.83$ for both T and $\chi = 0.48$ for $T = 4.0$ and 0.67 for $T = 3.0$. Note that at the Θ point, $T = 3.0$, χ is larger than the mean field prediction $\chi = 0.5$, due to fluctuations which lower T_Θ from its mean field value.

In the SCF,[9,51] the chemical potential, $\mu(z) = \partial f(\rho(z))/\partial\rho(z)$, should decay parabolically away from the grafting plane, whatever the form of $\rho(z)$. While this prediction cannot be checked directly, due to the difficulty in determining $\mu(z)$, it can be checked indirectly, in at least two ways. The first is to note that since

$$\Pi(z) = \rho(z)\,\mu(z) - f(\rho(z)) \qquad (7)$$

the partial derivative of both sides with respect to z gives

$$\frac{\partial\Pi(z)}{\partial z} = \rho(z)\frac{\partial\mu(z)}{\partial z} \qquad (8)$$

Therefore if $\mu(z)$ is parabolic, then $\rho(z)^{-1}(\partial\Pi(z)/\partial z)$ is linear in z. In addition, results for different ρ_a and N should fall on the same curve. While quite noisy due to the necessity of taking a numerical derivative, results for $\rho(z)^{-1}(\partial\Pi(z)/\partial z)$ for several ρ_a overlapped and were approximately linear, as shown in the inset to Figure 15. Another method is to use the Flory–Huggins form for the equation of state for $f(\rho(z))$ in eq 7 with the parameters fitted above and solve for $\mu(z)$. Results for $\mu(z)$ for a good solvent ($T = 4.0$) are shown in Figure 15. As predicted by the SCF theory, $\mu(z)$ decreases parabolically away from the grafting plane even when $\rho(z)$ does not. The slopes of these curves, particularly for small to intermediate z, are approximately the same, independent of ρ_a. Only for large z, where the data are less accurate, there are some deviations from the parabolic form, but I believe that these are due to the effect of finite N.

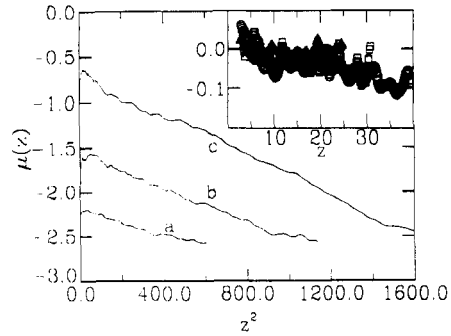

Figure 15. Chemical potential, $\mu(z)$, versus z^2 for $N = 100$ and $T = 4.0$ for the three values of Π_a and ρ_a presented in Figure 12. $\rho(z)^{-1}(\partial\Pi(z)/\partial z)$ versus z is shown in the inset for the values of $\Pi_a = 0.7$ (△), 4.7 (□), and 15.7 (○).

V. Summary

In this paper, I have presented the results of a constant surface pressure simulation for end-grafted polymer brushes under a range of solvent qualities for four chain lengths N and a wide range of grafting densities ρ_a. In contrast to previous simulations, the grafting density ρ_a is allowed to vary while the surface osmotic pressure Π_a is held fixed. This allows one to easily explore a wide range of surface densities by simply adjusting a single parameter. For both a good and Θ solvent, three regimes for the brush height h were found. In the low grafting density regime, $\rho_a < \rho_a^*$, the polymers only weakly overlap and h increases very slowly with ρ_a. For sufficiently long chains ($N \geq 100$ for the present model), there is a range of grafting densities where $h \sim N\,\rho_a^{1/3}$ as predicted by both scaling and SCF theories. For larger $\rho_a > \rho_{a1} \approx 0.12$, the monomer density reaches about half its bulk value and the scaling prediction breaks down as higher order interactions are important. For $N = 50$, $\rho_a^* \sim \rho_{a1}$ and by the time the brushes are sufficiently stretched to be in the scaling regime, higher order interactions are important. For chains of length $N = 50$ and 100, the height h was observed to depend on ρ_a approximately linearly over a wide range of ρ_a. This may explain the recent neutron reflectivity data of Factor *et al.*[28] for PS in a good solvent, who observed an apparently linear dependence of h on ρ_a instead of the expected scaling result $\rho_a^{1/3}$.

In addition to the brush height, which has been measured in all previous simulations, I also determined the dependence of the surface osmotic pressure Π_a on the grafting density ρ_a. In contrast to the scaling and SCF theories, I observed a stronger dependence of Π_a on ρ_a than predicted. For chain lengths N and grafting densities ρ_a where h scaled as expected (Figure 2), Π_a increased significantly more rapidly than expected by almost an extra power of ρ_a. While this result is not understood, it does agree with the recent experimental results of Kent *et al.*[27,50] and theoretical results of Carignano and Szleifer.[15,44] One explanation of this result is that Π_a is more sensitive to the finite volume of the monomers than the height h. The other is that there is something wrong with the theory of polymer brushes. However, since both the scaling and SCF theories give nearly the same prediction for Π_a, it is more likely that we have not yet reached the scaling regime for Π_a. This is possible since even though the grafting densities ρ_a studied were as low as 0.020, the monomer density $\rho(z)$ in the center of the brush was never less than about 0.12. This purely steric effect limits the interpretation of the chains and may explain the stronger depen-

dence of Π_a on ρ_a than predicted for the range of ρ_a accessible in the present simulation. Longer chains, probably of order 1000, would be necessary to determine for certain whether this explanation is correct. At present such simulations are not feasible.

The structure of the brush was also studied as a function of solvent quality. For fixed Π_a, the grafting density was observed to increase as the solvent quality decreased in such a way that the brush height h remained nearly constant. As seen in Figures 10 and 11, the monomer density profiles changed significantly as the solvent quality was decreased but h increased very little. For the highest grafting densities, h changed by less than about 10% even though T was changed over a wide range. In addition to the monomer density profile, the osmotic pressure $\Pi(z)$ and chemical potential $\mu(z)$ at height z away from the grafting plane were determined for the first time. $\Pi(z)/\rho(z)$ and $\mu(z)$ were both found to decrease parabolically as a function of z, even when $\rho(z)$ did not. The result for $\mu(z)$ is in agreement with the SCF theories.[9] Finally, the equation of state for monomers was determined and found, as expected, to depend only on the local monomer density $\rho(z)$.

Acknowledgment. I thank S. T. Milner, D. Perahia, and T. A. Witten for helpful discussions and I. Szleifer for allowing me to present some of his unpublished results[44] in Figure 3b.

References and Notes

(1) Milner, S. T. *Science* **1991**, *251*, 905.
(2) Napper, D. H. *Polymeric Stabilization of Colloidal Dispersions*; Academic: London, 1983.
(3) Alexander, S. *J. Phys. Fr.* **1977**, *38*, 983.
(4) de Gennes, P.-G. *Macromolecules* **1980**, *13*, 1069.
(5) Hirz, S. M.Sc. Thesis, University of Minnesota, 1987.
(6) Cosgrove, T.; Heath, T.; van Lent, B.; Leermakers, F.; Scheutjens, J. *Macromolecules* **1987**, *20*, 1692.
(7) Skvortsov, A. M.; Gorbunov, A. A.; Pavlushkov, I. V.; Zhulina, E. B.; Borisov, O. V.; Pryamitsyn, V. A. *Polym. Sci. USSR* **1988**, *30*, 1706.
(8) Muthukumar, M.; Ho, J.-S. *Macromolecules* **1989**, *22*, 965.
(9) Milner, S. T.; Witten, T. A.; Cates, M. E. *Macromolecules* **1988**, *21*, 2610; *Europhys. Lett.* **1988**, *5*, 413.
(10) Milner, S. T. *J. Chem. Soc., Faraday Trans.* **1990**, *86*, 1349.
(11) Zhulina, E. B.; Borisov, O. V.; Pryamitsyn, V. A. *J. Colloid Interface Sci.* **1990**, *137*, 495.
(12) Wijmans, C. M.; Scheutjens, J. M. H. M.; Zhulina, E. B. *Macromolecules* **1992**, *25*, 2657.
(13) Shim, D. F. K.; Cates, M. E. *J. Phys. Fr.* **1989**, *50*, 3535.
(14) Lai, P.-Y.; Halperin, A. *Macromolecules* **1991**, *24*, 4981.
(15) Carignano, M. A.; Szleifer, I. *J. Chem. Phys.* **1993**, *98*, 5006.
(16) Murat, M.; Grest, G. S. *Macromolecules* **1989**, *22*, 4054; *Phys. Rev. Lett.* **1989**, *63*, 1074; In *Computer Simulation of Polymers*; Roe, R. J., Ed.; Prentice-Hall: Englewood Cliffs, NJ, 1991; p 141.
(17) Chakrabarti, A.; Toral, R. *Macromolecules* **1990**, *23*, 2016; Chakrabarti, A.; Nelson, P.; Toral, R. *Phys. Rev. A* **1992**, *46*, 4930.
(18) Dickman, R.; Hong, D. C. *J. Chem. Phys.* **1991**, *95*, 4650.
(19) Lai, P.-Y.; Binder, K. *J. Chem. Phys.* **1991**, *95*, 9288.
(20) Taunton, J.; Toprakcioglu, C.; Fetters, L. J.; Klein, J. *Nature* **1988**, *332*, 712; *Macromolecules* **1990**, *23*, 571.
(21) Hadziioannou, G.; Patel, S.; Granick, S.; Tirrell, M. *J. Am. Chem. Soc.* **1986**, *108*, 2869.
(22) Patel, S. S.; Tirrell, M. *Annu. Rev. Phys. Chem.* **1989**, *40*, 597.
(23) Klein, J.; Perahia, D.; Warburg, S. *Nature* **1991**, *352*, 143.
(24) Cosgrove, T. *J. Chem. Soc., Faraday Trans.* **1990**, *86*, 1323.
(25) Auroy, P.; Auvray, L.; Leger, L. *Phys. Rev. Lett.* **1991**, *66*, 719; *Macromolecules* **1991**, *24*, 5158; Auroy, P.; Mir, Y.; Auvray, L. *Phys. Rev. Lett.* **1992**, *69*, 93.
(26) Field, J. B.; Toprakcioglu, C.; Ball, R. C.; Stanley, H. B.; Dai, L.; Barford, W.; Penfold, J.; Smith, G.; Hamilton, W. *Macromolecules* **1992**, *25*, 434.
(27) Kent, M. S.; Lee, L.-T.; Farnoux, B.; Rondelez, F. *Macromolecules* **1992**, *25*, 6240.
(28) Factor, B. J.; Lee, L.-T.; Kent, M. S.; Rondelez, F. *Phys. Rev. E* **1993**, *46*, R2354.
(29) Perahia, D.; Weisler, D.; Satija, S. K.; Fetters, L. J.; Sinha, S. K.; Milner, S. T., to be published.
(30) Halperin, A. *J. Phys. Fr.* **1988**, *49*, 547.
(31) Whitmore, M. D.; Noolandi, J. *Macromolecules* **1990**, *23*, 3321.
(32) Zhulina, E. B.; Borisov, O. V.; Pryamitsyn, V. A.; Birshtein, T. M. *Macromolecules* **1991**, *24*, 140.
(33) Ross, R. S.; Pincus, P. *Europhys. Lett.* **1992**, *19*, 79.
(34) Yeung, C.; Balazs, A. C.; Jasnow, D. *Macromolecules* **1993**, *26*, 1914.
(35) Huang, K.; Balazs, A. C. *Macromolecules* **1993**, *26*, 4736.
(36) Auroy, P.; Auvray, L. *Macromolecules* **1992**, *25*, 4134.
(37) Lai, P.-Y.; Binder, K. *J. Chem. Phys.* **1992**, *97*, 586.
(38) Grest, G. S.; Murat, M. *Macromolecules* **1993**, *26*, 3108.
(39) Winehold, J. D.; Kumar, S. K., to be published.
(40) Tang, H.; Szleifer, I., to be published.
(41) Lai, P.-Y. *J. Chem. Phys.* **1993**, *98*, 669.
(42) Granick, S.; Herz, J. *Macromolecules* **1985**, *18*, 460.
(43) de Gennes, P.-G. *Scaling Concepts in Polymer Physics*; Cornell University Press: Ithaca, NY, 1979.
(44) Carignano, M. A.; Szleifer, I., to be published.
(45) Andersen, H. C. *J. Chem. Phys.* **1980**, *72*, 2384.
(46) Parrinello, M.; Rahman, A. *Phys. Rev. Lett.* **1980**, *45*, 1196.
(47) Allen, M. P.; Tildesley, D. J. *Computer Simulation of Liquids*; Clarendon Press: Oxford, 1987.
(48) Kremer, K.; Grest, G. S. *J. Chem. Phys.* **1990**, *92*, 5057; **1991**, *94*, 4103 (erratum).
(49) Raphaël, E.; Pincus, P.; Fredrickson, G. H. *Macromolecules* **1993**, *26*, 1996.
(50) Kent, M. S.; Lee, L.-T.; Factor, B. J.; Rondelez, F.; Smith, G., to be published.
(51) Milner, S. T.; Witten, T. A., private communication, 1993.